

PAPER

A broadcast ephemeris design of LEO navigation augmentation satellites based on the integration-type ephemeris model

To cite this article: Lingdong Meng *et al* 2021 *Meas. Sci. Technol.* **32** 085009

View the [article online](#) for updates and enhancements.

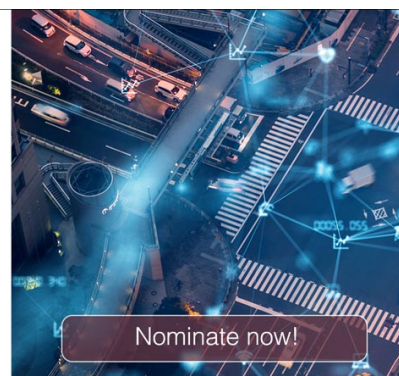


The Electrochemical Society
Advancing solid state & electrochemical science & technology


The ECS is seeking candidates to serve as the
Founding Editor-in-Chief (EIC) of ECS Sensors Plus,
a journal in the process of being launched in 2021

The goal of ECS Sensors Plus, as a one-stop shop journal for sensors, is to advance the fundamental science and understanding of sensors and detection technologies for efficient monitoring and control of industrial processes and the environment, and improving quality of life and human health.

Nomination submission begins: May 18, 2021



A broadcast ephemeris design of LEO navigation augmentation satellites based on the integration-type ephemeris model

Lingdong Meng^{1,2} , Junping Chen^{2,3,*}, Jiexian Wang¹ and Yize Zhang²

¹ College of Surveying and Geo-Informatics, Tongji University, Shanghai 200092, People's Republic of China

² Shanghai Astronomical Observatory, Chinese Academy of Sciences, Shanghai 200030, People's Republic of China

³ School of Astronomy and Space Science, University of Chinese Academy of Sciences, Beijing 100049, People's Republic of China

E-mail: junping@shao.ac.cn

Received 20 January 2021, revised 12 April 2021

Accepted for publication 22 April 2021

Published 21 May 2021



Abstract

Low Earth orbit (LEO) satellites are a promising type of navigation augmentation satellite for current global navigation satellite systems. Aiming at the navigation function, an effective broadcast ephemeris model needs to be designed for LEO satellites. An enhanced integration-type broadcast ephemeris model is proposed in this study. First, the short-term periodical variation characteristics of LEOs' accelerations in the Earth-centered Earth-fixed coordinate system are analyzed. The Chebyshev polynomials and harmonic functions are then applied to represent the variation perturbation of accelerations. Tests using simulated and real data from LEO satellites at altitudes from 600 to 1400 km are conducted to evaluate the fit accuracy of the proposed models in terms of arc length, integration method, integration step length, orbital altitude, inclination, eccentricity, etc. The fit accuracy is dramatically improved compared to that of the current GLONASS integration-type broadcast model, where fit errors less than 10 cm are achieved with an arc length of 20 min.

Keywords: LEO satellites, broadcast ephemeris model, GLONASS, augmentation satellites, integration, Runge–Kutta

(Some figures may appear in colour only in the online journal)

1. Introduction

Stable positioning, navigation and timing (PNT) services around the world are provided by current global navigation satellite systems (GNSSs). The Global Positioning System (GPS), Globalnaya Navigatsionnaya Sputnikovaya Sistema (GLONASS) and Galileo apply satellites operating in medium

Earth orbits (MEOs) to transmit navigation signals in the microwave band. The constellations of Beidou-2 and BeiDou-3 consist of geostationary orbit (GEO), inclined geostationary orbit (IGSO) and MEO satellites. Regional navigation satellite systems, such as the Japanese Quasi-Zenith Satellite System and the Indian Regional Navigation Satellite System also adopt IGSO and GEO satellites to provide PNT services. However, low Earth orbit (LEO) satellites, where the majority of operational satellites reside at altitudes of 300–1500 km [1], are not officially used for providing PNT service yet,

* Author to whom any correspondence should be addressed.

since the Navy Navigation Satellite System (TRANSIT) was retired.

In recent years, companies such as Orbcomm, Iridium, Globalstar, SpaceX and Boeing have been planning to launch and build commercial broadband LEO constellations consisting of hundreds or even thousands of LEO satellites. These satellites can provide broadband Internet services on a global scale and offer PNT services [2–5]. Moreover, the fully deployed Iridium Next constellation and the future Chinese Hongyan and Hongyun constellations have also included the function of navigation [6]. In 2018, the Luojia-1A scientific experimental satellite developed by Wuhan University carried a navigation augmentation payload and was launched with an orbital altitude of 647 km. Navigation signal augmentation from an LEO platform was successfully achieved by Luojia-1A [7, 8]. Compared to the current GNSSs satellites located in medium or high orbits, LEO satellites benefit from stronger signal strength and a faster speed, which is expected to provide a more robust PNT service in complex urban areas [9, 10]. Moreover, faster geometric variations from high-speed LEO satellites enable rapid precise point positioning (PPP) convergence and better ambiguity resolution [11–13]. Introducing LEO satellites into current GNSSs could improve PNT services significantly. To achieve this goal, one of the key prerequisites is to provide reliable broadcast ephemeris messages that meet the corresponding accuracy requirements for PNT services.

Broadcast ephemeris parameters are generated by the control segment according to corresponding observations. The GPS broadcast ephemeris, legacy navigation (LNAV), is based on the Kepler ephemeris model, which has been widely applied in BeiDou, QZSS and Galileo [14–17]. LNAV messages consist of 16 parameters to describe the operating status of MEO satellites. To obtain higher-accuracy orbital representations, another two parameters for the semimajor axis rate and the mean motion rate have been added to the new civil navigation (CNAV) message [18, 19]. GPS and QZSS transmit CNAV on L2 and L5 signals [20]. The Cartesian ephemeris model, including the position, velocity and acceleration at one specific epoch in the Earth-centered Earth-fixed (ECEF) coordinate system, is applied in GLONASS satellite orbital representations with an update interval of 30 min [21]. The ephemeris model of satellite-based augmentation systems is similar to that of GLONASS. The computation of GLONASS satellite positions uses numerical integration methods, such as the Runge–Kutta algorithm, which is very different from the user algorithms for a GPS LNAV or CNAV broadcast ephemeris message. The quality of the broadcast ephemeris is mainly affected in terms of model fit errors, orbit determination precision and propagation errors [22]. The quality of broadcast ephemeris has been assessed in various studies [23–27]. The orbit-only contribution to the user range error (URE) in 2014 was about 0.24, 0.54, 0.76, 0.50 and 0.57 m for GPS, GLONASS, Galileo, QZSS, BeiDou IGSO and MEO satellites, respectively [23]. The root mean square (RMS) of the fit URE is approximately 5–10 cm for MEO satellites with a 4 h arc length [28].

In recent years, the broadcast ephemeris representations of MEO, IGSO and GEO have been studied in terms of the design of the broadcast ephemeris model [29], the algorithm of ephemeris interpolation and parameter estimation [30–32], and the comparison of different ephemeris models [33–35]. With the rapid development of LEO constellation-augmented multi-GNSSs, it is necessary to carry out similar studies for the LEO satellite broadcast ephemeris. Unlike MEO, IGSO and GEO satellites, LEO satellites are closer to Earth, more easily influenced by higher-order gravity terms and have a shorter orbital period. Therefore, the orbit perturbation forces of LEO satellites are more complex. A typical broadcast ephemeris design has been realized in the retired TRANSIT system, whose constellation is composed of LEO satellites. The TRANSIT broadcast ephemeris consists of two parts: one is defined by Kepler-type elements with an update rate of 12 h and the other part is a set of corrections with an update rate of 2 min [36]. However, the model fit error is up to 5 m [37]. Obviously, this cannot satisfy the requirements of current PNT services. If the GPS LNAV broadcast ephemeris model is directly used to fit the LEO satellites at 400–1400 km altitudes, the arc length should be 10–20 min to match GPS 4 h fit accuracy [38]. Based on the GLONASS-type ephemeris model, improved integration-type broadcast models are recommended [39, 40], where quadratic polynomials and harmonic functions are used to fit satellite accelerations. However, the influence of orbital inclination and eccentricity is not considered. Although the Kepler-type ephemeris model is widely used in most GNSSs, for small orbital eccentricity or inclination, the Kepler orbital elements are usually singular [1, 41]. In order to solve the singularity problems caused by small orbital inclinations, a trade-off strategy has been proposed [28, 42–44]. In this strategy, the orbit of a GEO satellite is regarded as that of an IGSO satellite by intentionally adding 5° to the original small inclination and is then referred to as a pseudo-GEO. Users have to rotate back 5° of inclination to obtain the correct satellite positions. Therefore, in terms of procedure, this strategy is more complex and not the same as that for MEO and IGSO satellites. An even greater problem is that the fit accuracy of GEO satellites using this strategy is always worse than that of IGSO satellites [45] since singularities cannot be removed completely. The authors of [33, 35] have used non-singular elements to simultaneously remove the singularities caused by small inclinations and eccentricities of BeiDou GEO satellites. However, when the orbital inclination is larger, such as 90° , singularity still exists because the singularity in the perturbed motion equations are not avoided when the inclination is close to 90° . The authors of [22] have introduced another set of non-singular elements suitable for LEO satellites to remove the singularity caused by a small orbital eccentricity. However, their strategy fails when the orbital inclination is smaller, such as 0° , because for an orbital inclination close to zero, the right ascension of the ascending node is not well defined. As mentioned above, the current strategies to solve singularity problems are much more complex and cannot remove singularities completely.

Table 1. Detailed parameters of the LEO satellites.

Parameters	Value	
Orbital altitude	600 km	1000 km
Semimajor axis	6878.14 km	7378.14 km
Eccentricity	0.001	0.001
Inclination	45°	5°
Argument of perigee	0°	30°
Right ascension of ascending node (RAAN)	0°	0°
True anomaly	0°	0°
Data interval	60 s	
Duration	2019.04.27.00.00–2019.04.28.00.30	

In this study, we propose an enhanced integration-type broadcast ephemeris model suitable for LEO satellites. Benefiting from the non-singular character of the integration-type broadcast ephemeris model, singularities can be overcome completely. To enhance the fit accuracy of the LEO satellite representation, we propose extra parameters on the basis of the current GLONASS broadcast ephemeris model. In this paper, we describe the design and user algorithm of our proposed models. In the subsequent sections, we show our fit accuracy results considering many factors comprehensively. We discuss the effects of the arc length, orbital altitude, orbital inclination, orbital eccentricity, integration method and integration step on the fit accuracy and verify the effectiveness of our proposed ephemeris model using real LEO satellites in orbit.

2. LEO satellite broadcast ephemeris model design

The current integration-type broadcast ephemeris is designed for the GLONASS MEO satellites. Due to the violent effects of complex perturbations, this model cannot satisfy requirements in terms of orbit accuracy for PNT services using LEO satellites. As such, we consider some extra parameters in addition to the current GLONASS broadcast ephemeris model.

We use the Satellite Tool Kit (STK) software, a sophisticated space-analysis platform, to simulate the precise ephemeris of LEO satellites at 600 and 1000 km in high-precision orbit propagator mode. The detailed orbital parameters are listed in table 1. We analyze the characteristics of accelerations in the X, Y and Z directions in the ECEF coordinate system. The short-term periodical fluctuations of accelerations and spectrum analysis results for LEO satellites are illustrated in figures 1 and 2, respectively. Accelerations in the X, Y and Z directions show periodic oscillations with a period equivalent to approximately one per revolution and with trend variations to some degree.

For the current GLONASS broadcast model, the accelerations are regarded as constants in an effective period, which is suitable for MEO satellites. However, according to the results of the variation characteristics of the accelerations, extra

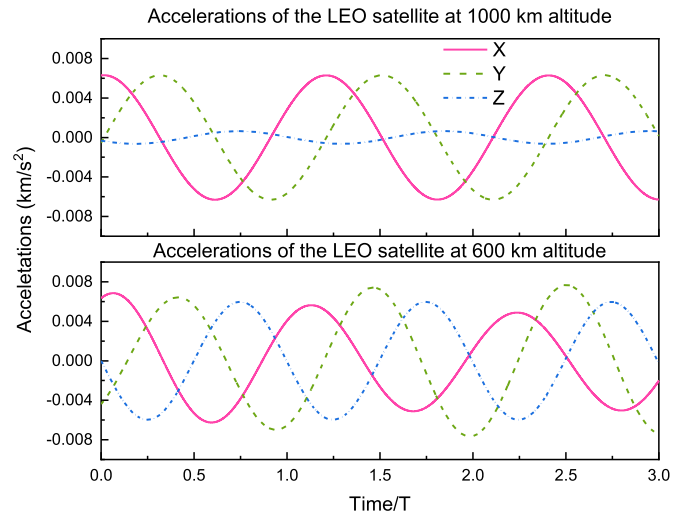


Figure 1. The short-term fluctuation of accelerations in the X, Y and Z directions in the ECEF coordinate system (three-orbit period).

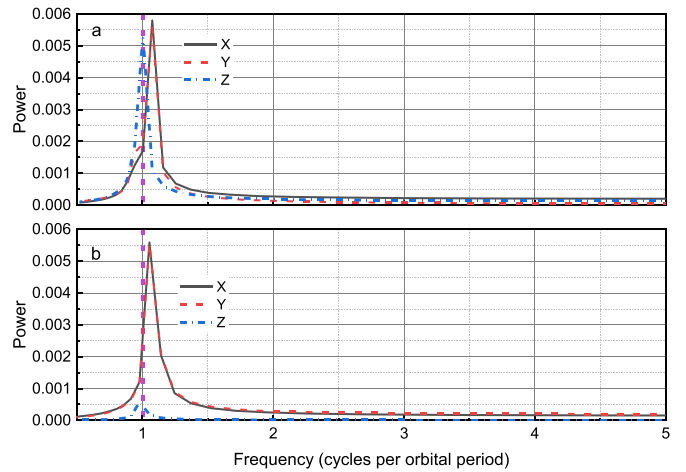


Figure 2. The spectral analysis results for LEO satellite orbits. (a) LEO satellite at a 600 km orbital altitude; (b) LEO satellite at a 1000 km orbital altitude.

parameters should be added to the current GLONASS broadcast model to represent complex variations [39, 40]. The first-order harmonic parameters can be considered as candidates to account for periodic variations. Moreover, due to the influence of atmospheric drag, LEO satellite positions show a gradually decreasing trend. Therefore, third- or second-order Chebyshev polynomials can be applied to represent trend variations. Based on these two approaches, four broadcast models are designed. The broadcast ephemeris parameters and their corresponding definitions for these four models are shown in tables 2–5.

2.1. The computation of satellite positions

Based on the above-mentioned broadcast ephemeris parameters, users can compute the satellite positions in the

Table 2. Parameter definitions for the integration-type broadcast ephemeris Model 1 for LEO satellites. This is the current GLONASS broadcast model.

Parameters	Definition
t_{oe}	The reference epoch
X, Y and Z	Satellite position at the reference epoch
V_x, V_y and V_z	Satellite velocity at the reference epoch
a_x, a_y and a_z	Accelerations in the X, Y and Z directions

Table 3. Parameter definitions for the integration-type broadcast ephemeris Model 2 for LEO satellites.

Parameters	Definition
t_{oe}	The reference epoch
X, Y and Z	Satellite position at the reference epoch
V_x, V_y and V_z	Satellite velocity at the reference epoch
a_x, a_y and a_z	Accelerations in the X, Y and Z directions
$(A_X, B_X), (A_Y, B_Y)$ and (A_z, B_z)	Harmonic parameters for acceleration in the X, Y and Z directions

Table 4. Parameter definitions for the integration-type broadcast ephemeris Model 3 for LEO satellites.

Parameters	Definition
t_{oe}	The reference epoch
X, Y and Z	Satellite position at the reference epoch
V_x, V_y and V_z	Satellite velocity at the reference epoch
C_{X0}, C_{X1}, C_{X2} and C_{X3}	Chebyshev polynomial coefficients for acceleration in the X direction
C_{Y0}, C_{Y1}, C_{Y2} and C_{Y3}	Chebyshev polynomial coefficients for acceleration in the Y direction
C_{Z0}, C_{Z1}, C_{Z2} and C_{Z3}	Chebyshev polynomial coefficients for acceleration in the Z direction

ECEF coordinate system according to given algorithms with equations (1)–(3), shown as follows:

$$\begin{aligned} \ddot{\mathbf{R}}_{\text{ECEF}_X} = & -\frac{GM}{r^3}X + \frac{3}{2}C_{20}\frac{GMa_e^2}{r^5}X\left(1 - \frac{5Z^2}{r^2}\right) \\ & + A_X \cos(n(t_{oe} - t)) + B_X \sin(n(t_{oe} - t)) \\ & + \omega^2X + 2\omega V_Y + \sum_{i=0}^3 C_{X_i}T_i(\tau), \end{aligned} \quad (1)$$

Table 5. Parameter definitions for the integration-type broadcast ephemeris Model 4 for LEO satellites.

Parameters	Definition
t_{oe}	The reference epoch
X, Y and Z	Satellite position at the reference epoch
V_x, V_y and V_z	Satellite velocity at the reference epoch
C_{X0}, C_{X1}, C_{X2} and C_{X3}	Chebyshev polynomial coefficients for acceleration in the X direction
C_{Y0}, C_{Y1}, C_{Y2} and C_{Y3}	Chebyshev polynomial coefficients for acceleration in the Y direction
C_{Z0}, C_{Z1} and C_{Z2}	Chebyshev polynomial coefficients for acceleration in the Z direction
$(A_X, B_X), (A_Y, B_Y)$ and (A_z, B_z)	Harmonic parameters for acceleration in the X, Y and Z directions

$$\begin{aligned} \ddot{\mathbf{R}}_{\text{ECEF}_Y} = & -\frac{GM}{r^3}Y + \frac{3}{2}C_{20}\frac{GMa_e^2}{r^5}Y\left(1 - \frac{5Z^2}{r^2}\right) \\ & + A_Y \cos(n(t_{oe} - t)) + B_Y \sin(n(t_{oe} - t)) \\ & + \omega^2X - 2\omega V_X + \sum_{i=0}^3 C_{Y_i}T_i(\tau), \end{aligned} \quad (2)$$

$$\begin{aligned} \ddot{\mathbf{R}}_{\text{ECEF}_Z} = & -\frac{GM}{r^3}Z + \frac{3}{2}C_{20}\frac{GMa_e^2}{r^5}Z\left(3 - \frac{5Z^2}{r^2}\right) \\ & + A_Z \cos(n(t_{oe} - t)) + B_Z \sin(n(t_{oe} - t)) \\ & + \sum_{i=0}^3 C_{Z_i}T_i(\tau), \end{aligned} \quad (3)$$

where GM is the product of the gravitational constant and Earth’s mass ($GM = 398\,600.44 \text{ km}^3 \text{ s}^{-2}$); r is the distance from the satellite to the mass center of Earth; a_e is the equatorial radius of Earth; ω is Earth’s rotation rate ($\omega = 0.7292115 \times 10^{-4} \text{ rad s}^{-1}$); C_{20} is the second zonal coefficient of the spherical harmonic expression ($C_{20} = -0.00108263$); C_{X_i}, C_{Y_i} and C_{Z_i} are Chebyshev polynomial coefficients for accelerations in the X, Y and Z directions. The recursive formula for $T_i(\tau)$ is:

$$\begin{cases} T_0(\tau) = 1 \\ T_1(\tau) = \tau \\ T_n(\tau) = 2\tau T_{n-1}(\tau) - T_{n-2}(\tau), \quad |\tau| \leq 1, n \geq 2, \end{cases} \quad (4)$$

where $\tau \in [-1, 1]$ can be transformed according to observation epoch t

$$\tau = \frac{2}{\Delta t}(t_{oe} - t), t \in [t_0, t_0 + \Delta t], \quad (5)$$

where Δt is the parameter arc length.

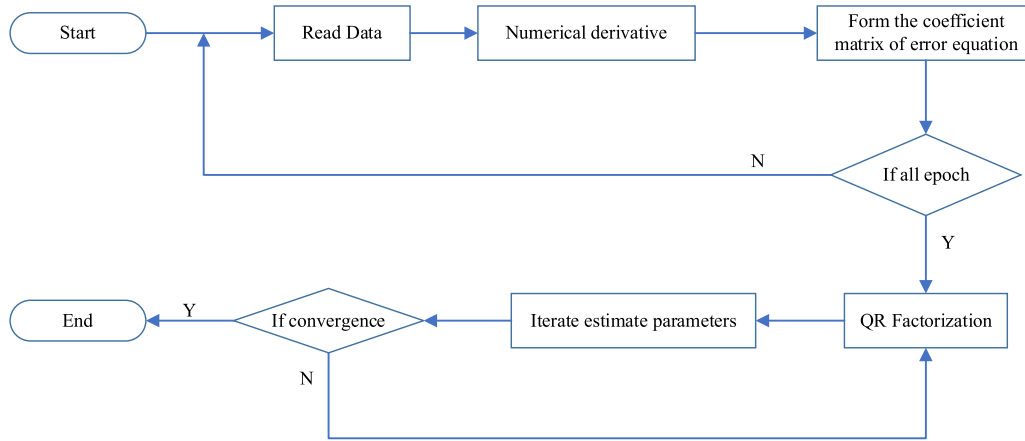


Figure 3. The process of fitting broadcast ephemeris parameters.

In the effective period for the broadcast ephemeris parameters, the satellite position and velocity at any observation epoch t can be calculated by using a numerical integration method, as follows:

$$\begin{cases} \dot{\mathbf{R}}_t = \dot{\mathbf{R}}_0 + \int_{t_{oe}}^t \ddot{\mathbf{R}}_{ECEF} dt \\ \mathbf{R}_t = \mathbf{R}_0 + \int_{t_{oe}}^t \dot{\mathbf{R}}_t dt, \end{cases} \quad (6)$$

where $\dot{\mathbf{R}}_0 = (V_X, V_Y, V_Z)^T$ and $\mathbf{R}_0 = (X, Y, Z)^T$ are the vectors of satellite velocity and position, respectively, at the reference epoch in the ECEF coordinate system; $\dot{\mathbf{R}}_t$ and \mathbf{R}_t are the vectors of satellite velocity and position, respectively, at any observation epoch in the ECEF coordinate system.

2.2. Parameter fitting

Generally speaking, the process of fitting parameters is similar to that of fitting Kepler-type broadcast ephemeris. The broadcast ephemeris parameters are generated using QR factorization and a numerical derivative method [1, 32]. Broadcast ephemeris parameters can be estimated using the least-squares method [33, 46]. However, the performance of the QR factorization approach is more stable in the case of near-singularity [1]. Moreover, the partial derivatives of each parameter should be calculated, and their structures are extremely complex. Therefore, in our study, the numerical derivative method [1] is used, which has been effectively used in generating GPS LNAV and BeiDou broadcast parameters [31, 32]. Although the numerical derivative is used for fitting the Kepler-type broadcast ephemeris in [31, 32], it is still suitable for the integration-type ephemeris.

The parameter-fitting process of our approach is illustrated in figure 3. First, the data for the predicted precise ephemeris are obtained. The numerical derivative method is then used to calculate the partial derivative. The coefficient matrix of the error equation is then formed. The process above is repeated until all the data for each epoch have been looped. Second, the estimated parameters are iterated using QR factorization

until convergence. Thus, the process of estimating the broadcast ephemeris is complete.

3. Results and discussion

We use STK to simulate the precise ephemeris of the LEO satellites at 600–1400 km orbital altitudes, which are applied to fit the broadcast ephemeris parameters. The simulated data for estimating the ephemeris parameters cover a period of approximately 24 h from 00:00:00 on 27 April 2019, to 00:30:00 on 28 April 2019. The data sample rate is set at 60 s. The performance of our proposed integration-type broadcast ephemeris model design for LEO satellites is comprehensively assessed considering the influence of numerical integration methods, the length of the integration step, orbital inclination, orbital eccentricity, arc length and orbital altitude. Three real LEO satellites in orbit, namely CryoSat-2, HY-2A and Jason-2, with a small orbital eccentricity and orbital altitude of about 720–1336 km were selected to validate our proposed broadcast ephemeris model.

3.1. The fit accuracy evaluation index

The orbit error Δr can be divided into three directions of radial (ΔR), along-track (ΔA) and cross-track (ΔC). The URE is an important index that reflects the impact of Δr on the user's line-of-sight vector [23]. For broadcast ephemeris parameter fitting, the fit errors should be no more than 10 cm [47]. The orbit-only contribution to the URE is defined as a weighted average of RMS errors $A = \text{RMS}(\Delta A)$, $C = \text{RMS}(\Delta C)$ and $R = \text{RMS}(\Delta R)$, as follows:

$$\text{URE} = \sqrt{w_R^2 R^2 + w_{A,C}^2 (A^2 + C^2)}. \quad (7)$$

The weight factors w_R and $w_{A,C}$ are positively related to the orbital altitude. For example, the w_R and $w_{A,C}$ for the GLONASS MEO satellites are 0.98 and 0.149, respectively; whereas, for the BeiDou GEO satellites, they are 0.99 and 0.089, respectively [23]. The values of the weight factors for

Table 6. URE weight factors for different orbital altitude LEO satellites.

Orbital altitude (km)	w_R	$w_{A,C}$
400	0.419	0.642
600	0.488	0.617
800	0.540	0.595
1000	0.582	0.575
1200	0.618	0.556
1400	0.648	0.539

LEO satellites from orbital altitudes 400–1400 km are listed in table 6 [22].

3.2. The comparison of different models

We use the four broadcast ephemeris models mentioned above to fit the precise ephemeris for the LEO satellite for which the orbital altitude is 1000 km, the inclination is 0° and the eccentricity is 0.001. In the process of fitting parameters, the fourth-order Runge–Kutta (RK-4) numerical integration method is used and the integration step is set at 30 s. The RMS fit accuracy results for these four models, which were designed in tables 2–5 are shown in tables 7 and 8.

In tables 7 and 8, the arc lengths of each fit batch are set to 20 min and 30 min, respectively. Based on the results, Model 4 achieves the best performance, while the GLONASS broadcast ephemeris model (Model 1) is the worst. The reason is that the short-term periodic signals and perturbation variations are fully considered in Model 4. The fit results also demonstrate that the singularity caused by small inclination and eccentricity is completely removed by our proposed models. Furthermore, when we increase the arc length from 20 to 30 min, the fit accuracy of Model 4 also decreases the least. Considering the stability and high accuracy, we propose Model 4 for the LEO broadcast ephemeris model. In the following sections, we will analyze the performance of Model 4.

3.3. The choice of numerical integration method

In an integration-type broadcast ephemeris model, a numerical integration method has to be used to calculate the satellite position and velocity at a specific observation epoch. Numerical integration methods can be classified into single-step and multistep methods [1]. Although multistep methods can achieve higher integration accuracy, they are more complex and time-consuming. Single-step methods, such as the widely used Runge–Kutta methods, are simple and can satisfy the requirements for the calculation of satellite position and velocity. We assessed the difference between third-order (RK-3), fourth-order (RK-4) and fifth-order (RK-5) Runge–Kutta algorithms with respect to fit accuracy. These Runge–Kutta algorithms are shown in equations (8)–(10), respectively. They are applied to fit parameters for an LEO satellite at a 1000 km altitude, of which the orbital eccentricity and inclination are 0.001 and

0°, respectively. The fit accuracy results and the RMS values of URE, R , A and C are given in tables 9 and 10:

$$\begin{cases} y_{n+1} = y_n + \frac{1}{6}(k_1 + 4k_2 + k_3) \\ k_1 = hf(x_n, y_n) \\ k_2 = hf\left(x_n + \frac{1}{2}h, y_n + \frac{1}{2}k_1\right) \\ k_3 = hf(x_n + h, y_n - k_1 + 2k_2) \end{cases}, \quad (8)$$

$$\begin{cases} y_{n+1} = y_n + \frac{1}{8}(k_1 + 3k_2 + 3k_3 + k_4) \\ k_1 = hf(x_n, y_n) \\ k_2 = hf\left(x_n + \frac{1}{3}h, y_n + \frac{1}{3}k_1\right) \\ k_3 = hf\left(x_n + \frac{2}{3}h, y_n - \frac{1}{3}k_1 + k_2\right) \\ k_4 = hf(x_n + h, y_n + k_1 - k_2 + k_3) \end{cases}, \quad (9)$$

$$\begin{cases} y_{n+1} = y_n + \frac{1}{24}k_1 + \frac{5}{48}k_4 + \frac{27}{56}k_5 + \frac{125}{336}k_6 \\ k_1 = hf(x_n, y_n) \\ k_2 = hf\left(x_n + \frac{1}{2}h, y_n + \frac{1}{2}k_1\right) \\ k_3 = hf\left(x_n + \frac{1}{2}h, y_n + \frac{1}{4}k_1 + \frac{1}{4}k_2\right) \\ k_4 = hf(x_n + h, y_n - k_2 + 2k_3) \\ k_5 = hf\left(x_n + \frac{2}{3}h, y_n + \frac{7}{27}k_1 + \frac{10}{27}k_2 + \frac{1}{27}k_4\right) \\ k_6 = hf\left(x_n + \frac{1}{5}h, y_n + (28k_1 - 125k_2 + 546k_3 + 54k_4 - 378k_5)\right) \end{cases}, \quad (10)$$

where y is the function value, x is the independent variable and h is the integration step.

As shown by tables 9 and 10, when the arc length is 20 min, the fit accuracy results are almost the same. However, when the arc length is 30 min, the fit accuracy of RK-3 is clearly worse than those of RK-4 and RK-5. The fit accuracy results of RK-4 and RK-5 are almost the same, but as shown by equations (9) and (10), RK-5 is clearly more complex. Therefore, the RK-4 numerical integration method is proposed to calculate satellite position and velocity at any observation epoch with respect to the design of a broadcast ephemeris model for LEO satellites.

3.4. The setting of numerical integration step length

The length of the numerical integration step affects parameter fit efficiency and the computational burden will be too heavy in the case of a short integration step. However, if the length is too long, the fit accuracy will decrease substantially. The relationships between fit accuracy and integration step length are illustrated in figure 4. The orbital eccentricity and orbital altitude are still set at 0.001 and 1000 km in this part, and the orbital

Table 7. Fit accuracy results using different models (arc length: 20 min; unit: m).

Model	User range error (URE)	Radial (R)	Along-track (A)	Cross-track (C)
Model 1	3.034	3.657	3.604	1.078
Model 2	0.186	0.221	0.225	0.060
Model 3	0.063	0.076	0.074	0.023
Model 4	0.011	0.013	0.013	0.006

Table 8. Fit accuracy results using different models (arc length: 30 min; unit: m).

Model	URE	R	A	C
Model 1	7.195	8.674	8.536	2.572
Model 2	0.796	0.950	0.948	0.302
Model 3	0.323	0.386	0.385	0.119
Model 4	0.068	0.079	0.079	0.048

Table 9. Fit accuracy using third- to fifth-order Runge–Kutta algorithms (arc length: 20 min; unit: meter).

Fit accuracy	RK-3	RK-4	RK-5
URE	0.015	0.011	0.011
R	0.018	0.013	0.013
A	0.017	0.013	0.013
C	0.006	0.006	0.006

Table 10. Fit accuracy using third- to fifth-order Runge–Kutta algorithms (arc length: 30 min; unit: meter).

Fit accuracy	RK-3	RK-4	RK-5
URE	0.122	0.068	0.068
R	0.152	0.079	0.079
A	0.15	0.079	0.079
C	0.048	0.048	0.048

inclination is 0°. Balancing between fit accuracy and computational efficiency, using 30 s as the integration step length is recommended.

3.5. The influence of orbital inclination and eccentricity

To investigate the influence of orbital inclination and eccentricity on the orbit fit accuracy, we simulate different satellite orbits with orbital inclinations varying from 0° to 90°, with orbital eccentricity and altitude set at 0.001 and 1000 km. Thus, all cases of inclination that may appear in the future LEO constellation design were considered. The URE RMS values of the fit accuracy as a function of the orbital inclination are shown in figure 5. When the arc length is 20 min, the fit accuracy is still stable; however, when the arc length is 30 min, the fit accuracy changes largely.

In order to assess the effect of orbital eccentricity on the fit accuracy, the orbital inclination and altitude are set at 45° and 1000 km. The orbital eccentricity varies from 0.001 to 0.030. The relationships between fit accuracy and orbital eccentricity

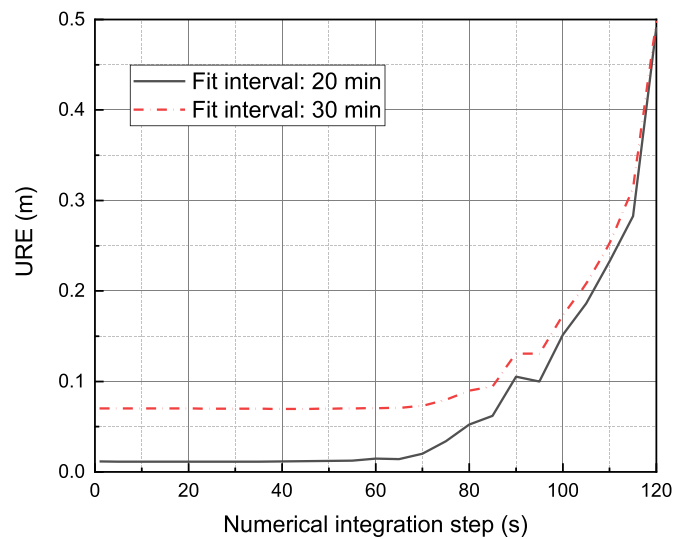


Figure 4. Relationships between integration step and RMS values of fit accuracy.

are shown in figure 6. Although the orbital eccentricity varies, the fit accuracy is still stable.

From the fit accuracy results, we conclude that the singularities caused by small eccentricities and small or large inclinations can be overcome by the integration-type ephemeris model.

In comparison, using the broadcast ephemeris model proposed in [22], although singularities caused by small eccentricities can be removed, a singularity still exists when the inclination is 0°. Using the models in [33, 35], the singularity caused by a small inclination can be solved; however, the singularity problem still exists when the inclination is close to 90°. These problems are due to singularities arising from the definition of some of the orbital elements [1]. This is because the perigee itself is not well defined for an almost circular orbit. In other words, the argument of perigee is not a meaningful orbital element for small eccentricities. Nor is the RAAN when the orbital inclination is close to 0°. However, an integration-type broadcast ephemeris model is completely immune to these troublesome singularity problems.

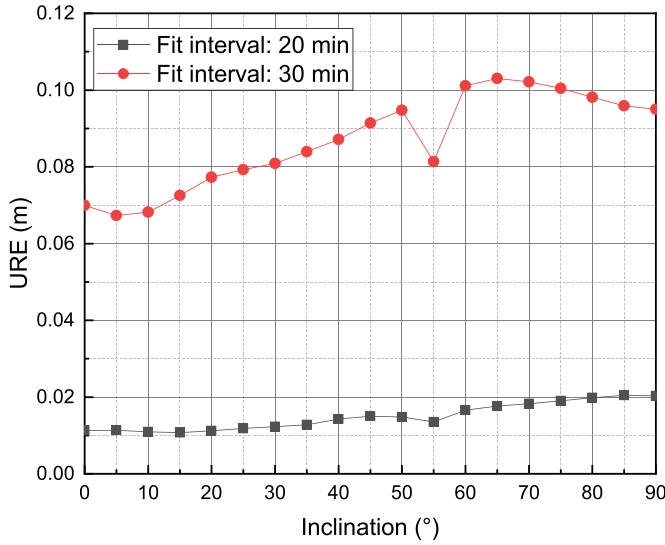


Figure 5. RMS values of fit accuracy as a function of the orbital inclination.

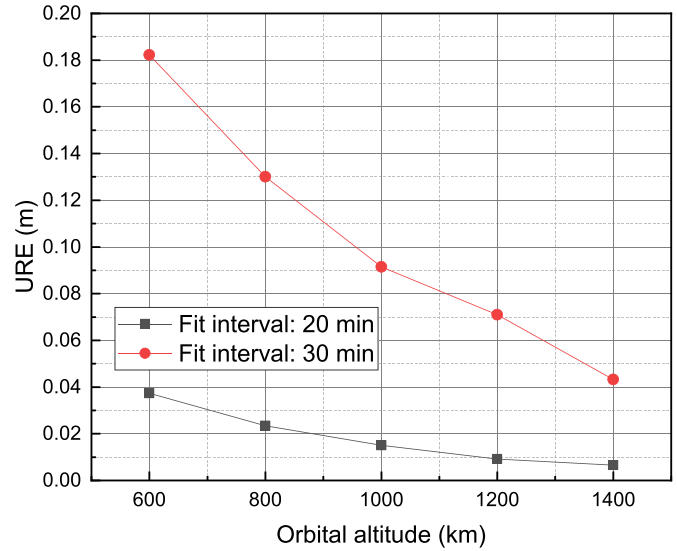


Figure 7. RMS values of fit accuracy as a function of orbital altitude.

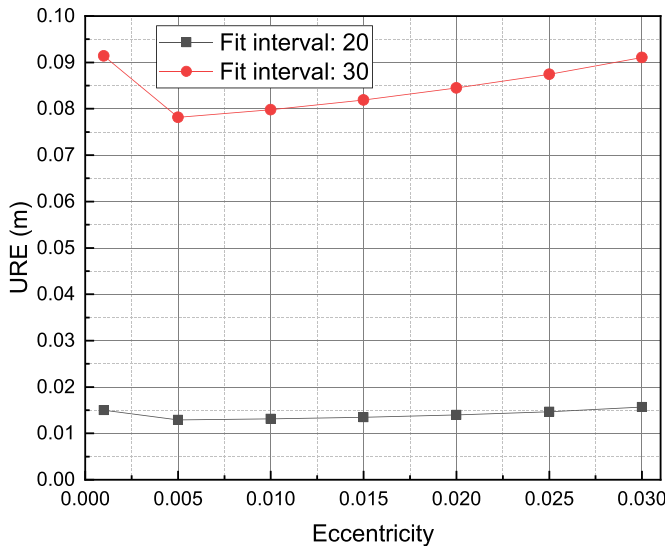


Figure 6. RMS values of fit accuracy as a function of orbital eccentricity.

To achieve the convergence of the orbit fit, the number of iterations for the enhanced integration-type broadcast ephemeris model is approximately 3–5. However, since parameters are highly related to each other for the Kepler-type broadcast model, it needs at least 7–8 iterations to achieve convergence [31].

3.6. The influence of orbital altitude

To investigate the influence of orbital altitude on the orbit fit. We simulate the orbital inclination and eccentricity as 45° and 0.001, and orbital altitudes vary from 600 to 1400 km. As illustrated in figure 7, satellites with higher orbit altitudes achieve more precise fit accuracy. When the orbital altitudes are higher

than 1000 km and the arc length is 20 min, the URE RMS values are smaller than 1 cm. Overall, when using our proposed model with an arc length of 20 min for LEO satellites with altitudes ranging from 600 to 1400 km, their URE RMS values are no more than 4 cm.

3.7. Validation from real LEO satellites

All the experiments mentioned above are performed based on the simulated precise ephemeris. Three real LEO satellites (CryoSat-2, HY-2A and Jason-2) with orbital altitudes from approximately 720 to 1336 km and a data sample rate of 60 s are used to validate our proposed model. The specific orbital parameters are listed in table 11. Their orbital eccentricities are all very close to zero.

Figure 8 illustrates the RMS values of fit UREs for three real LEO satellites. Similar to the simulated results, the higher the orbital altitude, the better the fit accuracy. Although the orbital eccentricities are very close to zero, the singularities caused by small eccentricities are resolved and broadcast ephemeris parameters can still be generated successfully. We consider the influence of the arc length on the fit accuracy when the arc length is 20 min and the URE RMS values are no more than 4 cm.

Figure 9 shows the time series of fit errors for the LEO satellite, Jason-2. For an arc length of 20 min, the fit errors in all three directions are within ±6.5 cm and the UREs are no more than 5.1 cm. When the arc length is 30 min, the fit errors in all three directions are within ±39 cm and the UREs are no more than 31 cm. Therefore, the orbital altitude and arc length have highly significant influences on the fit accuracy, which is also reflected in the experimental results based on the simulated precise ephemeris.

Table 11. Basic orbital information for real LEO satellites for broadcast ephemeris validation.

Name	Inclination	Eccentricity	Altitude (km)	Data (yyyy.mm.dd.hh.mm-hh.mm)
CryoSat-2	92°	0.000	720	2010.07.25.00.00–23.59
HY-2A	99.35°	0.00117	971	2012.08.11.00.00–23.59
Jason-2	66°	0.000	1300	2009.08.13.00.00–23.59

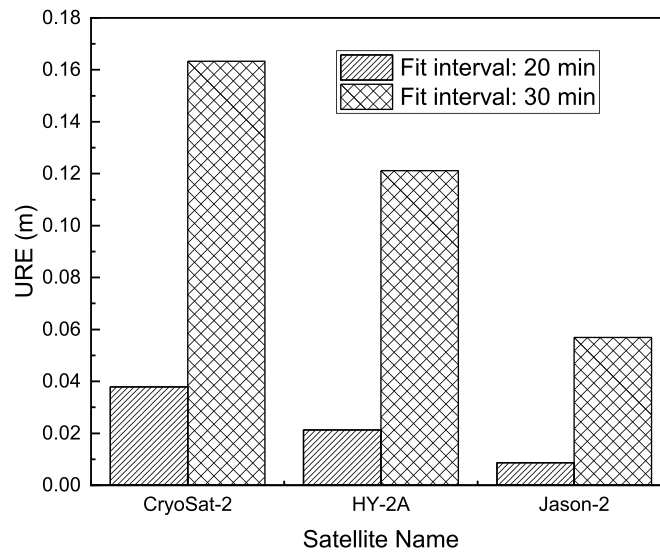


Figure 8. RMS values of fit accuracy of three real LEO satellites in orbit.

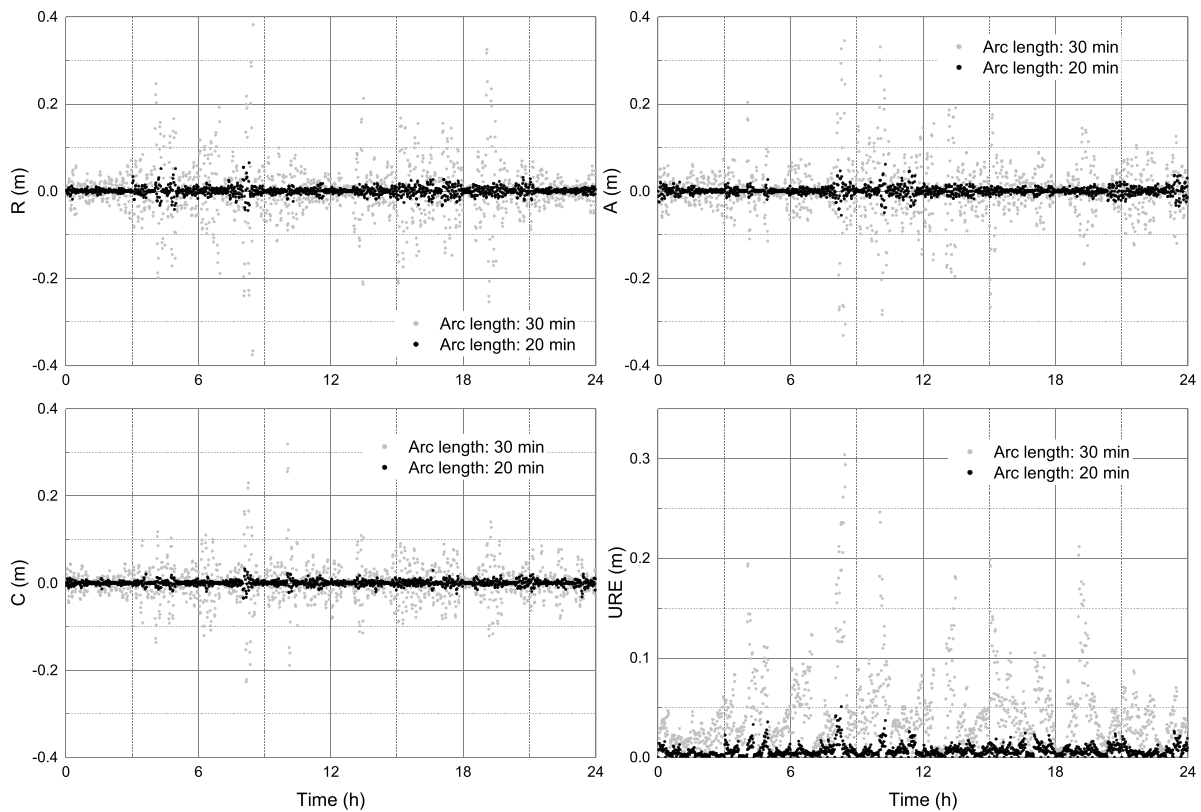


Figure 9. Time series of fit error distribution in the along-track (*A*), cross-track (*C*) and radial (*R*) directions as well as fit UREs for the real LEO satellite, Jason-2. The fuscous and light-colored points represent fit errors of 20 and 30 min arc length, respectively.

4. Conclusions

As a consequence of very short orbital periods and more complex orbit perturbed motions, it is challenging to represent LEO satellites operating statuses with high precision. Almost all current studies on broadcast ephemeris models focus on MEO, IGSO and GEO satellites. In this paper, we present a broadcast ephemeris model for LEO satellites based on the integration-type model. Compared with Kepler-type models that suffer accuracy degradation in the case of singularity problems, our proposed strategy is completely immune to these problems.

The reliability of our proposed broadcast ephemeris model is assessed using both simulated and real precise ephemeris. The impacts in terms of the numerical integration method, the length of the numerical integration step, the arc lengths, the orbital altitude, the orbital eccentricity and the orbital inclination are discussed in detail. The experimental results show that fit UREs are dramatically improved with an increase in orbital altitude and a shortening of arc lengths. Benefiting from non-singularity characteristics that are superior to Kepler-type broadcast ephemeris modes, problems due to the singularities caused by small orbital eccentricity and small or larger orbital inclination can be completely resolved.

In addition to the design of the broadcast ephemeris model and the arc length, other aspects, such as the design of the interface of the broadcast ephemeris model, the message size, the precision of the predicted orbit and clock error, and users' time-to-first-fix, are also of deep significance as regards an effective broadcast ephemeris design for navigation systems. In future studies, these factors will be carefully considered.

Data availability statements

The simulated data is available upon request. The real LEO satellite data can be downloaded in <ftp://doris.ign.fr>.

No new data were created or analysed in this study.

Acknowledgments

This research is supported by the National Natural Science Foundation of China (Grant No. 11673050); the Key Program of Special Development funds of Zhangjiang National Innovation Demonstration Zone (Grant No. ZJ2018-ZD-009), the National Key R&D Program of China (Grant No. 2018YFB0504300), and the Key R&D Program of Guangdong Province (Grant No. 2018B030325001).

ORCID iD

Lingdong Meng  <https://orcid.org/0000-0003-1118-328X>

References

- [1] Montenbruck O and Gill E 2000 *Satellite Orbits: Models, Methods, and Applications* (Berlin: Springer Berlin Heidelberg) (<https://doi.org/10.1007/978-3-642-58351-3>)
- [2] Li X *et al* 2019 LEO constellation-augmented multi-GNSS for rapid PPP convergence *J. Geod.* **93** 749–64
- [3] Li B, Ge H, Ge M, Nie L, Shen Y and Schuh H 2019 LEO enhanced Global Navigation Satellite System (LeGNSS) for real-time precise positioning services *Adv. Sp. Res.* **63** 73–93
- [4] Joerges M, Gratton L, Pervan B and Cohen C E 2010 Analysis of Iridium-augmented GPS for floating carrier phase positioning *Navig. J. Inst. Navig.* **57** 137–60
- [5] Ma F *et al* 2020 Hybrid constellation design using a genetic algorithm for a LEO-based navigation augmentation system *GPS Solut.* **24** 62
- [6] Meng Y *et al* 2018 A global navigation augmentation system based on LEO communication constellation 2018 *European Navigation Conf. (ENC), (May 2018)* pp 65–71
- [7] Lei W, Ruizhi C, Deren L, Baoguo Y and Cailun W 2018 Quality assessment of the LEO navigation augmentation signals from Luojia-1A satellite *Geomatics Inf. Sci. Wuhan Univ.* **43** 2191–6
- [8] Lei W *et al* 2018 Initial assessment of the LEO based navigation signal augmentation system from Luojia-1A satellite *Sensors* **18** 3919
- [9] Ge H *et al* 2018 Initial assessment of precise point positioning with LEO enhanced global navigation satellite systems (LeGNSS) *Remote Sens.* **10** 984
- [10] Rabinowitz M and Spilker J J 2005 A new positioning system using television synchronization signals *IEEE Trans. Broadcast.* **51** 51–61
- [11] Li X *et al* 2019 Improved PPP ambiguity resolution with the assistance of multiple LEO constellations and signals *Remote Sens.* **11** 408
- [12] Li X, Lv H, Ma F, Li X, Liu J and Jiang Z 2019 GNSS RTK positioning augmented with large LEO constellation *Remote Sens.* **11** 16
- [13] Tian S, Dai W, Liu R, Chang J and Li G 2014 System using hybrid LEO-GPS satellites for rapid resolution of integer cycle ambiguities *IEEE Trans. Aerosp. Electron. Syst.* **50** 1774–85
- [14] CSNO 2013 BeiDou navigation satellite system signal in space interface control document-open service signal, Version 2 (China Satellite Navigation Office (CSNO))
- [15] GPS Directorate 2013 Navstar GPS space segment/navigation user interfaces, Interface (Global Positioning Systems Directorate)
- [16] EU 2015 European GNSS (Galileo) open service signal in space interface control document, Issue 1.2 (European Union)
- [17] JAXA 2014 *Quasi-Zenith satellite system navigation service interface specification for QZSS IS-QZSS V1.6* Japan Aerospace Exploration Agency
- [18] Steigenberger P, Montenbruck O and Hessels U 2015 Performance evaluation of the early CNAV navigation message *Navigation* **62** 219–28
- [19] Wang A, Chen J, Zhang Y, Wang J and Wang B 2019 Performance evaluation of the CNAV broadcast ephemeris *J. Navig.* **72** 1331–44
- [20] Yin H, Morton Y T, Carroll M and Vinande E 2015 Performance analysis of L2 and L5 CNAV broadcast ephemeris for orbit calculation *Navig. J. Inst. Navig.* **62** 121–30
- [21] ICD-GLONASS 2016 Global navigation satellite system GLONASS, interface control document, general description

- of code division multiple access signal system, Edition 1 (Russian Institute of Space Device Engineering)
- [22] Xie X, Geng T, Zhao Q, Liu X, Zhang Q and Liu J 2018 Design and validation of broadcast ephemeris for low Earth orbit satellites *GPS Solut.* **22** 54
- [23] Montenbruck O, Steigenberger P and Hauschild A 2015 Broadcast versus precise ephemerides: a multi-GNSS perspective *GPS Solut.* **19** 321–33
- [24] Warren D L M and Raquet J F 2003 Broadcast vs. precise GPS ephemerides: a historical perspective *GPS Solut.* **7** 151–6
- [25] Lv Y, Geng T, Zhao Q, Xie X and Zhou R 2020 Initial assessment of BDS-3 preliminary system signal-in-space range error *GPS Solut.* **24** 16
- [26] Montenbruck O, Steigenberger P and Hauschild A 2018 Multi-GNSS signal-in-space range error assessment—methodology and results *Adv. Sp. Res.* **61** 3020–38
- [27] Wang Z, Shao W, Li R, Song D and Li T 2018 Characteristics of BDS signal-in-space user ranging errors and their effect on advanced receiver autonomous integrity monitoring performance *Sensors* **18** 4475
- [28] Fu X and Wu M 2012 Optimal design of broadcast ephemeris parameters for a navigation satellite system *GPS Solut.* **16** 439–48
- [29] Reid T G R, Walter T, Enge P K and Sakai T 2016 Orbital representations for the next generation of satellite-based augmentation systems *GPS Solut.* **20** 737–50
- [30] Horemuž M and Andersson J V 2006 Polynomial interpolation of GPS satellite coordinates *GPS Solut.* **10** 67–72
- [31] Wang J and Wang J 2014 Fitting and extrapolating accuracy of GPS broadcast ephemeris *J. Liaoning Tech. Univ. Sci.* **33** 1118–22
- [32] Wang J, Wang J, Chen J and Broadcast Ephemeris B D S 2016 Fitting based on satellite's position and velocity *J. Tongji Univ. Natural Sci.* **44** 155–60
- [33] Lan D, Zhongkai Z, Jin Z, Li L, Rui G and Feng H 2015 An 18-element GEO broadcast ephemeris based on non-singular elements *GPS Solut.* **19** 49–59
- [34] Diesposti R et al 2004 The proposed state vector representation of broadcast navigation message for user equipment implementation of GPS satellite ephemeris propagation *Proc. 2004 National Technical Meeting of the Institute of Navigation January 26–28, 2004 the Catamaran Resort Hotel San Diego, CA (January)* pp 294–312
- [35] Zhang Z, Du L, Liu L, He F, Lu Y and Zhou P 2014 Parameter design of GEO broadcast ephemeris based on the nonsingular orbital elements *Acta Geod. Cartogr. Sin.* **43** 452–7
- [36] Thomas S J 1968 The navy navigation satellite system: description and status *Navigation* **15** 229–43
- [37] Piscane V L, Holland B B and Black H D 1973 Recent (1973) improvements in the navy navigation satellite system *Navigation* **20** 224–9
- [38] Reid T G R, Neish A M, Walter T F and Enge P K, Leveraging commercial broadband LEO constellations for navigation *The 29th Int. Technical Meeting of the Satellite Division of the Institute of Navigation (ION GNSS+ 2016, Pp 2300–2314) (Portland, Oregon, USA, 12–16 September 2016, no. October)*
- [39] Lu Y, Du L, Zhang Z K and Zhou P Y 2015 Enhanced orbit catalogue ephemeris and its application in BeiDou mixed constellation *Yuhang Xuebao/J. Astronaut.* **36** 804–10
- [40] Fang S, Du L, Zhou P, Lu Y, Zhang Z and Liu Z 2016 Orbital list ephemerides design of LEO navigation augmentation satellite *Acta Geod. Cartogr. Sin.* **45** 904–10
- [41] Xu G and Xu J 2013 On the singularity problem in orbital mechanics *Mon. Not. R. Astron. Soc.* **429** 1139–48
- [42] Ruan R, Jia X, Wu X and Feng L 2011 Broadcast ephemeris parameters fitting for GEO satellites based on coordinate transformation *Acta Geod. Cartogr. Sin.* **40** 145–50
- [43] Guo R, Zhou J, Hu X, Liu L, Huang Y and Chang Z 2011 A strategy of rapid orbit recovery for the geostationary satellite *Acta Geod. Cartogr. Sin.* **40** 19–25
- [44] Cui X, Yang Y and Wu X 2012 Influence of the orbital plane rotation angle on GEO satellite broadcast ephemeris parameter fitting *J. Astronaut.* **33** 590–6
- [45] Choi J H, Kim G, Lim D W and Park C 2020 Study on optimal broadcast ephemeris parameters for GEO/IGSO navigation satellites *Sensors* **20** 6544
- [46] Zhou P, Yang H, Xiao G, Du L and Gao Y 2019 Estimation of GPS LNAV based on IGS products for real-time PPP *GPS Solut.* **23** 27
- [47] U. S. Department Of Defense 2008 *Global Positioning System Standard Positioning Service* www.Gps.Gov, September, pp 1–160 (available at: www.gps.gov/technical/ps/2008-SPS-performance-standard.pdf)